Toxicology Research

PAPER

View Article Online
View Journal | View Issue

Cite this: *Toxicol. Res.*, 2019, **8**, 206

Effects of long-term exposure to aluminum in the hippocampus in the type 2 diabetes model rats

Sung Min Nam,[a,b] Dae Young Yoo,[a] Hyun Jung Kwon,[c] Jong Whi Kim,[a] Hyo Young Jung,[a] Dae Won Kim,[c] Je Kyung Seong,[a,d] In Koo Hwang [a,d] and Yeo Sung Yoon *[a,d]

We investigated the long-term effects of aluminum (Al) exposure in the hippocampus in Zucker diabetic fatty (ZDF) rats and Zucker lean control (ZLC) rats. Six-week-old ZLC and ZDF rats were randomly divided into Al- and non-Al-groups. They were sacrificed 27 weeks after Al exposure (2000 ppm) through drinking water. Al exposure did not affect physiological parameters such as the body weight and blood glucose levels, but the prolonged diabetic condition had significant effects on the body weight and blood glucose levels. To determine the effects of diabetes and Al exposure on the neural plasticity and inflammatory response in the hippocampus, we examined the levels of doublecortin (DCX), *N*-methyl-D-aspartate receptors (NMDAR1, NMDAR2A, and NMDAR2B), and ionized calcium-binding adapter molecule 1 (Iba-1) in the hippocampus. DCX immunohistochemical staining revealed that Al exposure significantly reduced neuronal differentiation in both ZLC and ZDF rats. In particular, ZDF rats showed significantly decreased DCX immunoreactive neuroblasts compared with ZLC rats after aluminum exposure. In contrast, the expression of postsynaptic NMDARs was altered only in ZDF–Al rats; the protein expression level of NMDAR1 was reduced, but that of NMDAR2B increased in the hippocampus. Iba-1-immunoreactive microglia with morphological changes, including increased cytoplasm and retracted processes, were detected in the long-term diabetic condition and in the case of the co-existence of diabetes and Al exposure. Al exposure aggravated the diabetes-induced reduction of neuroblast differentiation and NMDAR signaling and facilitated the morphological changes associated with inflammatory activation in microglia in the hippocampus. However, further studies are still needed to confirm these findings.

Received 19th July 2018,
Accepted 21st November 2018

DOI: 10.1039/c8tx00192h

rsc.li/toxicology-research

Introduction

Zucker diabetic fatty (ZDF) rats have been widely used as a characteristic rodent model of type 2 diabetes mellitus (T2DM), and high-risk genetic factors (leptin receptor [*Lepr*] deficiency) involved in the onset of diabetes in ZDF rats. T2DM is an underlying disease with multiple complications, such as atherosclerosis, hypertension, stroke, retinopathy, heart attack, nephropathy, cognitive impairments, and neurodegenerative diseases.[1] With regard to the quality of life, chronic T2DM-induced cognitive impairment is regarded as an important early clinical sign of dementia involving brain degeneration.[2] The accumulated impairment of adult neurogenesis and subsequent neuronal loss in the hippocampus lead to cognitive dysfunction. The loss of brain neuronal cells is closely related to insulin levels, and diabetes enhances neuronal losses in the ischemic brain.[3,4] Neuronal losses in the hippocampi in aged individuals and patients with Alzheimer's disease (AD) have also been identified.[5] In addition, the structural reduction of newly generated neurons and synaptogenesis, alteration in the brain energy metabolism, and subsequent functional cognitive impairments are important contributors to diabetes-induced neurodegeneration.[6,7] Epidemiological studies reveal that the rate of the co-existence of T2DM and AD increases in an age-dependent manner,[8,9] and chronic sustained disease aggravates both conditions.[10] However, few studies have examined the mutual relationship between T2DM and dementia and the underlying mechanisms.

Aluminum (Al) is a non-essential element in mammals but helps in healthy growth in some organisms such as plants. Humans ingest approximately 30–50 mg of Al per day because

[a]*Department of Anatomy and Cell Biology, College of Veterinary Medicine, and Research Institute for Veterinary Science, Seoul National University, Seoul 08826, South Korea. E-mail: ysyoon@snu.ac.kr; Fax: +82 2 8711752; Tel: +82 2 8801264*
[b]*Department of Anatomy, College of Veterinary Medicine, Konkuk University, Seoul 05030, Republic of Korea*
[c]*Department of Biochemistry and Molecular Biology, Research Institute of Oral Sciences, College of Dentistry, Gangneung-Wonju National University, Gangneung 25457, South Korea*
[d]*KMPC (Korea Mouse Phenotyping Center), Seoul National University, Seoul 08826, South Korea*

of its environmental abundance and wide usage in daily life.[11] Additionally, Al exposure has been found as one of the environmental factors contributing to dementia. Al treatment triggers AD-like pathology in a D-galactose-induced aging mouse model.[12] Al accumulation, especially in the brain, has been demonstrated to increase the load of amyloid beta peptides.[12,13] Moreover, high-fat diets and diabetes predispose the development of AD pathology.[14,15] However, the effect of long-term Al exposure on the brains in T2DM animal models has not been investigated to date.

The hippocampus is susceptible to diabetes-induced impairment, and AD pathology starts developing early in the hippocampus before spreading to the neocortex.[16] Absorbed Al can be transported to all brain regions with the highest concentration being found in the hippocampus.[17] Diverse effects of Al exposure on synaptic plasticity can be observed from parturition throughout life, and the lactation period is the most susceptible to the Al-induced impairment of synaptic plasticity.[18] In the present study, we hypothesized that long-term exposure to Al facilitates diabetes-induced impairments of synaptic plasticity. Because leptin-receptor deficient ZDF rats show obesity and hyperglycemia earlier than Goto-Kakizaki rats,[19] the ZDF ($Lepr^{fa/fa}$) and the healthy Zucker lean control (ZLC, $Lepr^{+/+}$) rats were used in this study. This study aimed at investigating the long-term effect of Al exposure through drinking water on the plasticity of the hippocampus in a T2DM rat model, in which the hippocampus is susceptible to Al and/or type 2 diabetes-induced impairments.

Materials and methods

Experimental animals

Male and female heterozygous types ($Lepr^{fa/+}$) of ZDF rats were acquired from Genetic Models Co. (Indianapolis, ME, USA) and were mated with each other to get homozygous ZDF and ZLC rats. The rats were housed in a conventional state at adequate temperature (23 °C) and under humidity (60%) control with a 12 h light/12 h dark cycle, and they were allowed free access to tap water and diet (Purina 5008, Purina Korea, Korea) as recommended by Genetic Models Co. Animal handling and care conformed to the guidelines established by the current international laws and policies (NIH Guide for the Care and Use of Laboratory Animals, NIH Publication No. 85-23, 1985, revised 2011) and were approved by the Institutional Animal Care and Use Committee of Seoul National University (Approval No.: SNU-140219-1). All of the experiments were conducted to minimize the number of animals used and the suffering caused by the procedures in the present study.

Genotyping of the $Lepr^{fa}$ gene and the experimental design

The genotype of the $Lepr^{fa}$ gene herein was determined with the protocol described in our previous study.[20] To investigate the effects of long-term Al exposure on the neuronal plasticity and microglial response in the diabetic hippocampus, male rats were randomly divided into four groups: ZLC, Al-supplied ZLC (ZLC–Al), ZDF, and Al-supplied ZDF (ZDF–Al) groups (n = 10 per group, 5 rats for histological analysis and the other 5 rats for immunoblotting). In humans, oral and/or drinking water exposure is a more reasonable way of Al exposure than the intraperitoneal injection for Al exposure. Therefore, we adopted drinking water as a way of Al exposure.[21] Aluminum chloride ($AlCl_3$, Sigma, St Louis, MO, USA) was dissolved in deionized water (pH 6.7). Studies have demonstrated that after rats are exposed to a low concentration of Al (20 ppm, 1.7 mg kg^{-1} daily) in drinking water from 12 months of age for 22 months, AD phenotypes can be induced in these rats in old age.[22] In addition, albino Wistar rats show AD-like cognitive impairments after the oral administration of a high concentration of Al (200 mg kg^{-1}) in combination with D-galactose treatment.[23] Because of the increased death rate of ZDF rats (more than 50%) after the age of 1 year, we used a higher concentration of Al (2000 ppm) in young rats in this study. Under these conditions, Al can effectively accumulate in the brain and cause brain dysfunction without increasing mortality.[24,25] At 6 weeks of age, ZLC–Al and ZDF–Al rats received Al in drinking water for 27 weeks. All animals were euthanized at 33 weeks of age (Fig. 1A).

Body weight and blood glucose levels

To evaluate the chronic effects of co-existent Al exposure and diabetes on physiological parameters, we measured the body weight and blood glucose (fed glucose, not fast glucose) levels on the last day of the experiment. Blood was sampled in the morning (9:00 a.m.) by "tail nick" using a 27 G needle and the blood glucose levels were measured with a portable glucose monitor (ACCU-CHEK® GO; Roche, Mannheim, Germany).

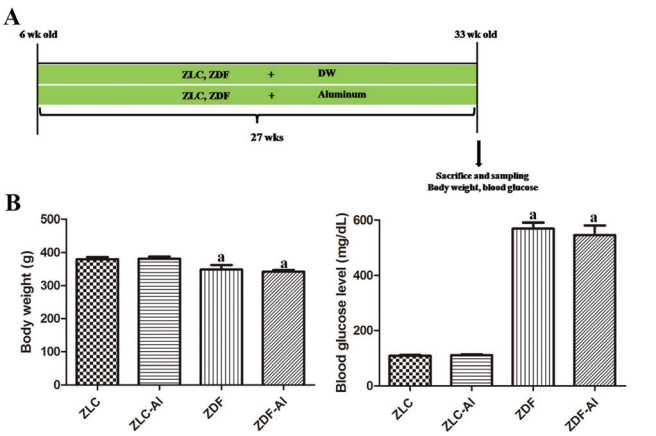

Fig. 1 Experimental design (A), blood glucose levels and body weights (B) in Zucker lean control (ZLC), aluminum-treated ZLC (ZLC–Al), Zucker diabetic fatty (ZDF), and aluminum-treated ZDF (ZDF–Al) rats. Differences between the means were analyzed using two-way analysis of variance (n = 10 per group; [a] $P < 0.05$, indicates a significant difference between ZLC and ZDF or between ZLC–Al and ZDF–Al groups). No significant differences were detected between ZLC and ZLC–Al or ZDF and ZDF–Al groups. Error bars indicate the standard error of means (SEM).

Tissue processing for histology

Animals in each group (n = 5 per group) were anesthetized with 1.5 g kg^{-1} urethane (Sigma) and were perfused transcardially with 0.1 M phosphate-buffered saline (PBS, pH 7.4) followed by 4% paraformaldehyde in 0.1 M phosphate buffer (pH 7.4). The pancreases and brains were removed and post-fixed in 4% paraformaldehyde for 12 h. For insulin immunohistochemistry and hematoxylin and eosin (H&E) staining, the pancreatic tissues were dehydrated with graded concentrations of alcohol and xylene and were then embedded in paraffin. Subsequently, 4 μm-thick sections were serially cut using a microtome (Leica, Wetzlar, Germany), and these sections were mounted onto silane-coated slides (Muto-glass, Tokyo, Japan). The pancreas sections were stained with H&E staining according to the general protocol. For the immunohistochemical staining of neuroblast and microglia markers, the brains were cryoprotected by infiltration with 30% sucrose for 1–2 days. Following equilibration in 30% sucrose in PBS, the brains were serially cut into 30 μm-thick coronal sections using a cryostat (Leica, Wetzlar, Germany). The sections were then collected into a six-well plate containing PBS for further process.

Immunohistochemistry

In order to obtain accurate data, immunohistochemical staining was carefully conducted under the same conditions. Three pancreatic tissue sections were selected for each animal. In brief, the sections were placed in a 400 mL jar filled with citrate buffer (pH 6.0) and were heated in a microwave oven (Optiquick Compact, Moulinex) operating at a frequency of 2.45 GHz and 800 W power setting. After three heating cycles (5 min each), slides were allowed to cool at room temperature and were washed in PBS. Free-floating brain sections were carefully processed under the consistent conditions to obtain accurate data for immunohistochemistry. The brain sections were selected between −3.00 and −4.08 mm to the bregma in reference to the rat atlas for each animal,[26] and a total of 10 brain sections (90 μm apart) were used in the present study. The sections were sequentially treated with 0.3% hydrogen peroxide in PBS for 30 min and 10% normal goat or horse serum in 0.05 M PBS for 30 min. The sections were then incubated with the diluted guinea-pig anti-insulin antibody (1 : 200, Abcam, Cambridge, UK) for the pancreas, and the goat anti-doublecortin (DCX) antibody (1 : 50, SantaCruz Biotechnology, Santa Cruz, CA, USA) or the rabbit anti-ionized calcium-binding adapter molecule 1 (Iba-1) antibody (1 : 1000, Wako, Osaka, Japan) for the brain overnight at room temperature. Subsequently, the sections were exposed to biotinylated goat anti-guinea-pig IgG, horse anti-goat IgG, or goat anti-rabbit IgG and the streptavidin–peroxidase complex (1 : 200, Vector, Burlingame, CA, USA). They were then visualized by the reaction with 3,3′-diaminobenzidine tetrachloride (Sigma) in 0.1 M Tris-HCl buffer (pH 7.2) and were mounted on gelatin-coated slides. After dehydration, the sections were mounted in a toluene based-mounting medium (Richard-Allan Scientific, Thermo Scientific).

The numbers of DCX- and Iba-1-positive cells in all groups were counted using an image analysis system equipped with a computer-based CCD camera (Optimas 6.5 software, CyberMetrics, Scottsdale, AZ, USA).

Analysis of a region of interest in the hippocampal proper was performed using an image analysis system. Images were calibrated into an array of 512 × 512 pixels corresponding to a tissue area of 140 × 140 μm (40× primary magnification). Each pixel resolution was 256 gray levels. The intensity of DCX, insulin, and Iba-1 immunoreactivity was evaluated by means of a relative optical density (ROD), which was obtained after the transformation of the mean gray level using the following formula: ROD = log (256/mean gray level). Using the NIH Image 1.59 software, the ROD of the background was determined in unlabeled portions, and the value was subtracted for correction, yielding high ROD values in the presence of preserved structures and low values after a structural loss. A ratio of the ROD was calibrated as a percentage.

Western blotting analysis

To investigate the effects of Al and diabetes on *N*-methyl-D-aspartate receptors (NMDAR1, NMDAR2A, and NMDAR2B) in the hippocampus, the other 5 rats in each group were sacrificed by decapitation and were used for western blotting analysis. After the brain was removed, the hippocampus was dissected with a surgical blade and stored at −80 °C for further analysis. The tissues were homogenized in 50 mM PBS (pH 7.4) containing 0.1 mM ethylene glycol bis(2-aminoethyl ether)-*N*,*N*,*N*′,*N*′ tetraacetic acid (pH 8.0), 0.2% Nonidet P-40, 10 mM ethylenediamine tetraacetic acid (pH 8.0), 15 mM sodium pyrophosphate, 100 mM β-glycerophosphate, 50 mM NaF, 150 mM NaCl, 2 mM sodium orthovanadate, 1 mM phenylmethylsulfonyl fluoride, and 1 mM dithiothreitol (DTT). After centrifugation, the supernatants were collected, and the protein level was determined using a Micro BCA protein assay kit with bovine serum albumin as the standard (Pierce Chemical, Rockford, IL, USA). Aliquots containing 40 μg of the total protein were boiled in the loading buffer containing 150 mM Tris (pH 6.8), 3 mM DTT, 6% sodium dodecyl sulfate, 0.3% bromophenol blue, and 30% glycerol. The aliquots were then loaded onto a polyacrylamide gel. After electrophoresis, the gel was transferred to a nitrocellulose transfer membrane (Pall Corp., East Hills, NY). To reduce background staining, the membrane was incubated with 5% non-fat dry milk in PBS containing 0.1% Tween 20 for 45 min, followed by incubation with rabbit anti-NMDAR1 (1 : 1000; Millipore, Temecula, CA, USA), rabbit anti-NMDAR2A (1 : 1000; Thermo Fisher Scientific), or rabbit anti-NMDAR2B (1 : 1000; Millipore) antibodies. Subsequently, the peroxidase-conjugated anti-rabbit IgG solution and an enhanced luminol-based chemiluminescent (ECL) kit (Pierce Chemical) were used. Thereafter, the blotted membranes were densitometrically scanned to quantify the ROD of each band using the NIH Image 1.59 software. The data were normalized against β-actin.

Statistical analysis

The data shown here represent the means of experiments performed for each experimental region. Differences among the means were statistically analyzed by two-way analysis of variance followed by Bonferroni post-tests in order to evaluate the differences among the groups.

Results

Body weight and blood glucose levels

Body weights and blood glucose levels were significantly higher at the early stage of diabetes in the ZDF and ZDF–Al groups than in the ZLC or ZLC–Al group (data not shown), but body weights were significantly lower in the ZDF group than those in the ZLC group after chronic progression of diabetes. Long-term Al exposure did not affect the body weights in either ZLC or ZDF rats (Fig. 1B). Notably, the state of hyperglycemia persisted until the end of the experiment (Fig. 1B). The blood glucose levels in ZLC and ZLC–Al rats were 106.00 and 110.25 mg dL^{-1}, respectively; however, the blood glucose in ZDF and ZDF–Al rats remained at high levels of 569.67 and 546.00 mg dL^{-1}, respectively. The blood glucose levels did not show any significant alterations after Al exposure in ZLC and ZDF rats (Fig. 1B).

Pancreatic histology

H&E staining revealed that pancreatic islets were compact and oval shaped in the ZLC group (Fig. 2A), and insulin immunoreactive cells (β cells) were easily observed throughout the pancreatic islets (Fig. 2B). In addition, no histological and immunohistochemical differences for insulin were observed between ZLC and ZLC–Al groups, and β cells were scattered throughout the islet in the ZLC–Al group (Fig. 2C and D). However, islets were significantly hypertrophied and irregular in shape with an apparent reduction in β cells in the ZDF group (Fig. 2E, F, and I). In ZDF rats, β cells were mainly detected in the periphery of the islet. No histological differences were found between the ZDF–Al group and the ZDF group (Fig. 2G), and β cells were sparsely dispersed across the rim of the islet in the ZDF–Al group (Fig. 2H and I). The ROD of insulin-immunoreactive β cells and the size of the pancreatic islets showed a similar change pattern. Diabetes significantly reduced the insulin immunoreactivity, but Al exposure did not (Fig. 2I).

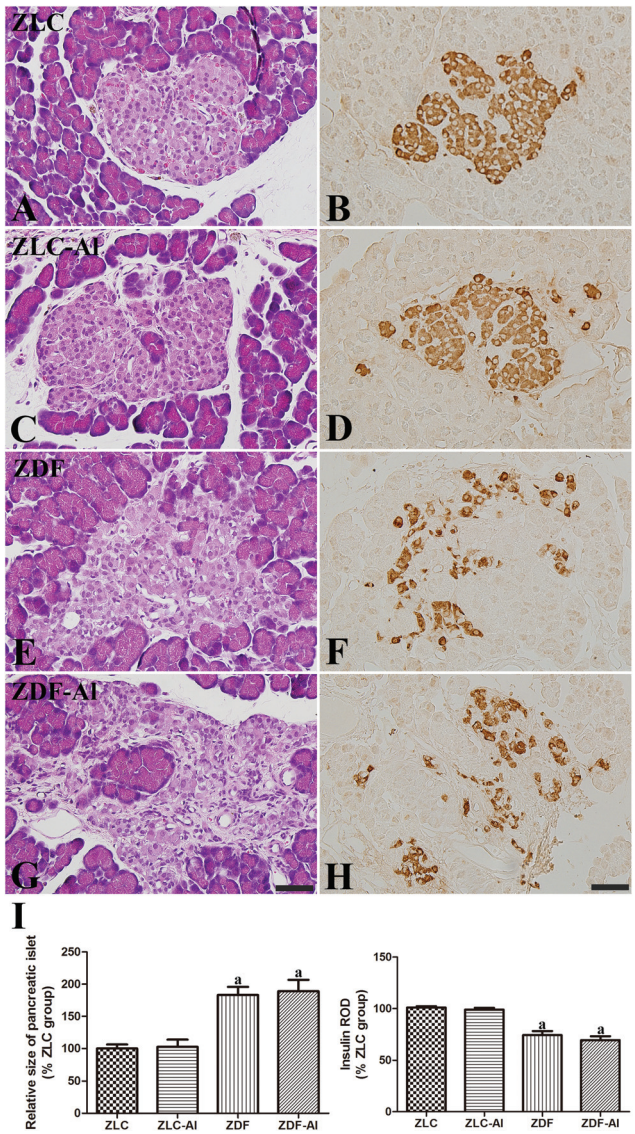

Fig. 2 Hematoxylin and eosin staining (A, C, E and G) and immunohistochemistry for insulin (B, D, F and H) in the pancreatic islets in the ZLC (A and B), ZLC–Al (C and D), ZDF (E and F), and ZDF–Al (G and H) rats. Scale bar = 50 μm. The relative size of the pancreatic islets and insulin immunoreactivity are expressed as percentages of the respective values in the ZLC group (I). Note that the islets are significantly enlarged in ZDF and ZDF–Al groups and insulin immunoreactive β cells are decreased in the ZDF and ZDF–Al rats. However, no histological and immunohistological differences are found between non-Al and Al groups (n = 5 per group; [a] $P < 0.05$ indicates a significant difference between ZLC and ZDF or ZLC–Al and ZDF–Al groups, [b] $P < 0.05$ indicates a significant difference between ZLC and ZLC–Al or ZDF and ZDF–Al groups). Error bars indicate the SEM.

Effects of Al on neuronal differentiation in ZLC and ZDF rats

DCX immunoreactive neuroblasts were observed in the subgranular zone and the lower granule cell layer of the dentate gyrus in all groups (Fig. 3). DCX immunoreactive cells were more easily detected in the ZLC group than in other groups, and their dendrites were well developed and had high complexity in the ZLC group (Fig. 3A and B). However, in the ZLC–Al group, the number of DCX immunoreactive cells was lower, and the cells showed impaired dendritic branching (Fig. 3C, D, and I). In the ZDF group, the chronic diabetic condition negatively affected the number and dendritic branching of DCX immunoreactive cells; DCX immunoreactive cells were scantly detected, and the complexity of dendrites markedly decreased (Fig. 3E, F, and I). Moreover, the numbers of DCX immunoreactive neuroblasts were significantly reduced and dendritic fibers were the most poorly developed relatively in the ZDF–Al group (Fig. 3G and H). These findings of DCX immunoreactivity suggest the additive harmful effects of Al and diabetes (Fig. 3H).

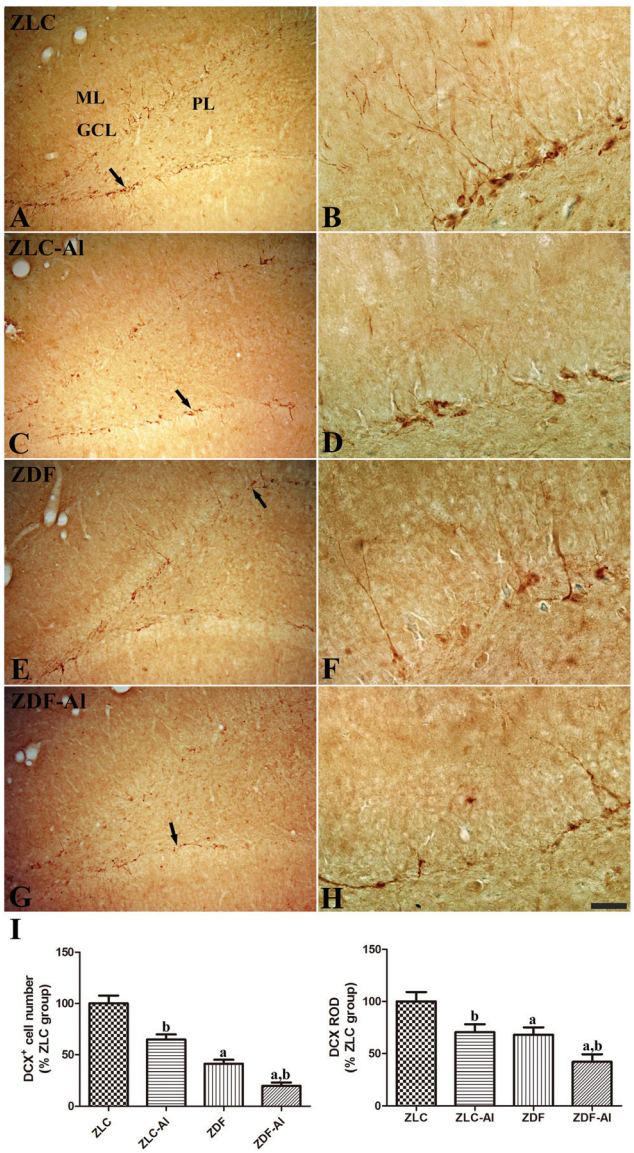

Fig. 3 Immunohistochemistry for doublecortin (DCX) in the dentate gyrus in ZLC (A and B), ZLC–Al (C and D), ZDF (E and F), and ZDF–Al (G and H) rats. Scale bar = 100 μm (A, C, E, and G), or 25 μm (B, D, F, and H). DCX-immunoreactive neuroblasts are observed in the subgranular zone (arrows) of the dentate gyrus. Note that DCX-immunoreactive neuroblasts are decreased in the ZLC–Al and ZDF–Al groups compared with ZLC and ZDF groups, respectively. The lowest number of DCX-immunoreactive neuroblasts is observed in the ZDF–Al group. GCL, granule cell layer; PL, polymorphic layer; ML, molecular layer. (I) Relative number and relative optical density (ROD) of DCX-immunoreactive neuroblasts are presented as percentages of the respective values in the ZLC group (n = 5 per group; [a] $P < 0.05$ indicates a significant difference between ZLC and ZDF or ZLC–Al and ZDF–Al groups, [b] $P < 0.05$ indicates a significant difference between ZLC and ZLC–Al or ZDF and ZDF–Al groups). The error bars indicate the SEM.

Effects of Al on microglia in the hippocampus in ZLC and ZDF rats

In all groups, Iba-1 immunoreactive microglial cells were observed in the polymorphic and molecular layer of the hippocampal dentate gyrus. In the ZLC group, the majority of Iba-1 immunoreactive microglia had a small soma with ramified processes (Fig. 4A). In the ZLC–Al group, Iba-1 immunoreactive microglia in the dentate gyrus of the hippocampus seemed to be morphologically unchanged (Fig. 4B), and the numbers of Iba-1 immunoreactive microglia were similar in ZLC and ZLC–Al groups (Fig. 4E). The ZDF rats showed an altered morphology of Iba-1 immunoreactive microglia, including the hypertrophied cytoplasm and retracted processes, compared with the ZLC rats (Fig. 4C). Notably, the numbers of Iba-1 immunoreactive microglia in the dentate gyrus were similar in the ZDF and ZLC rats (Fig. 4E). Iba-1 immunoreactivity significantly increased in the dentate gyrus in the ZDF rats compared with the ZLC rats. In the ZDF–Al group, the Iba-1 immunoreactive microglia in the polymorphic and molecular layer of the dentate gyrus were in the activated round form and had hypertrophied cytoplasm (Fig. 4D). The total numbers of

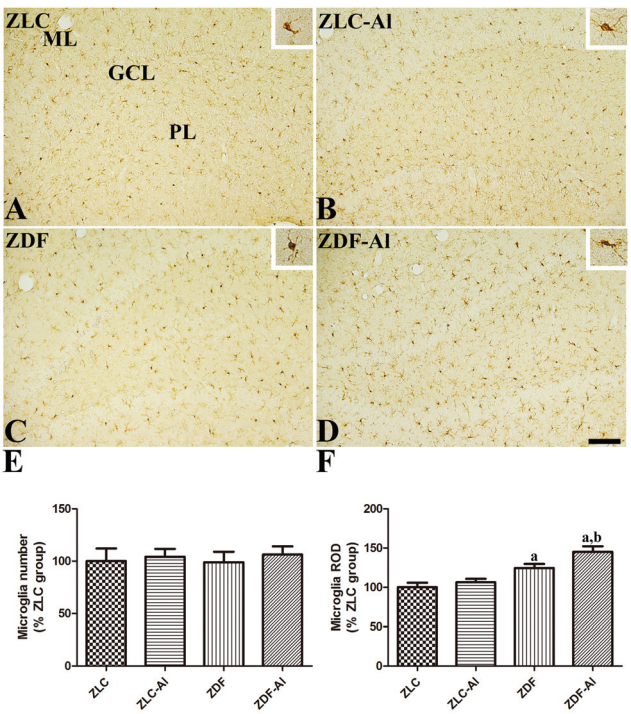

Fig. 4 Ionized calcium-binding adapter molecule 1 (Iba-1) immunoreactivity in the dentate gyrus in ZLC (A), ZLC–Al (B), ZDF (C), and ZDF–Al (D) rats. Iba-1 immunoreactivity is mainly detected in the polymorphic layer (PL) and the molecular layer (ML) of the dentate gyrus in the hippocampus. Iba-1 immunoreactive microglia in ZLC and ZDF rats have less ramified processes than those in ZLC–Al and ZDF–Al rats (inset image). These morphological changes are more prominent in the ZDF–Al group than in the ZLC–Al group. However, there are no significant differences in the number of Iba-1 immunoreactive cells between groups. GCL: granule cell layer. Scale bar = 100 μm. (E) Relative number and the ROD of Iba-1 immunoreactive microglia in the dentate gyrus in the hippocampus are expressed as percentages of the respective values in the ZLC group (n = 5 per group; [a] $P < 0.05$ indicates a significant difference between ZLC and ZDF or ZLC–Al and ZDF–Al groups, [b] $P < 0.05$ indicates a significant difference between ZLC and ZLC–Al or ZDF and ZDF–Al groups). The error bars indicate the SEM.

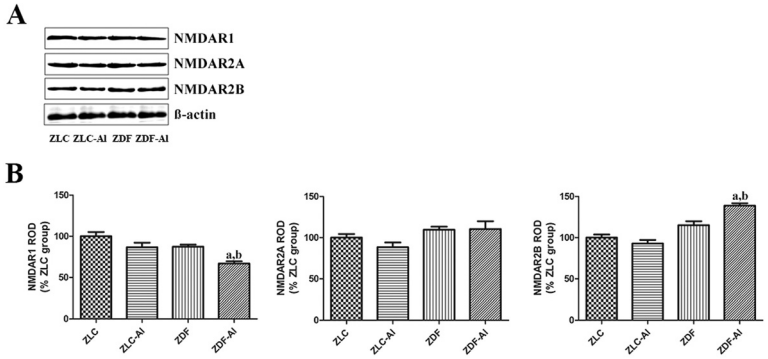

Fig. 5 Western blotting analysis of *N*-methyl-D-aspartate receptors (NMDAR1, NMDAR2A, and NMDAR2B) in the hippocampus in the ZLC, ZLC–Al, ZDF, and ZDF–Al groups. The ROD of immunoblot bands is expressed as a percentage of the value in the ZLC group (n = 5 per group; [a] $P < 0.05$ indicates a significant difference between ZLC and ZDF or ZLC–Al and ZDF–Al groups, [b] $P < 0.05$ indicates a significant difference between ZLC and ZLC–Al or ZDF and ZDF–Al groups). The error bars indicate the SEM.

microglia were not prominently different between the ZDF–Al and the ZDF groups (Fig. 4E), but Iba-1 immunoreactivity significantly increased in the ZDF–Al group compared with the ZDF group (Fig. 4E).

Effects of Al on NMDARs in the hippocampus in ZLC and ZDF rats

The expression levels of NMDARs, including the essential NMDAR1 subtype and auxiliary NMDAR2A and NMDAR2B subtypes, did not significantly differ in the hippocampus between ZLC and ZDF groups. Additionally, Al exposure did not apparently affect the NMDAR expression in ZLC rats. However, the expression level of NMDAR1 was significantly reduced in the ZDF–Al group compared with the ZDF group, but the expression level of NMDAR2B significantly increased in the ZDF–Al group compared with the ZDF group (Fig. 5).

Discussion

ZDF rats are prone to obesity and T2DM due to their characteristic hypothalamic leptin resistance and subsequent dysregulation in feeding suppression.[27,28] Additionally, peripheral leptin insensitivity in the pancreatic islets in ZDF rats causes lipogenesis and fat overload in the pancreas, leading to β cell dysfunction and the development of diabetes.[29] Our previous study has demonstrated that Al exposure for 10 weeks potentiates diabetes-induced impairment of adult hippocampal neurogenesis.[25] The present study investigated the effects of long-term Al exposure (27 weeks) on the hippocampus.

We examined the body weight and blood glucose levels in the experimental groups prior to the experiment. Although the body weight was lower in 33 week-old ZDF rats (at the chronic diabetic stage) than in age-matched ZLC rats, ZDF rats were overweight at the early stage of diabetes.[25] The converse change in the body weight is thought to be caused by prolonged diabetes in ZDF rats. This loss in the body weight is also found in the chronic stage of T2DM and T1DM.[30,31] Besides weight loss, polyuria, polydipsia, and polyphagia are induced by hyperglycemia in DM.[32] In the present study, hyperglycemia persisted until the later stage of diabetes regardless of Al exposure. The present results of pancreatic histology are similar to those in a previous study, which found that *db*/*db* mice had hypertrophy, an irregular shape of pancreatic islets, and an altered distribution pattern of β cells.[33] Compared with *db*/*db* mice, the ZDF rats showed an apparent reduction in insulin immunoreactivity in our study. However, long-term Al exposure did not lead to significant changes in the pancreatic morphology and β cell distribution in both ZLC and ZDF rats.

Next, we investigated the effects of chronic diabetes and Al exposure on neuroblast differentiation in the hippocampus. DCX is the microtubule-binding protein that is required for microtubule polymerization and stabilization.[34] DCX-regulated cytoskeletal dynamics are important in neuronal migration and differentiation, and DCX is widely used as a marker of neuroblasts and early neurons.[34,35] Both diabetes and Al treatment reduced the expression of DCX, and the co-existence of diabetes and Al exposure aggravated the reduction. Our previous studies demonstrated that the administration of Al exacerbated the reduction in cell proliferation and neuronal differentiation in the hippocampus in the mice fed a high-fat diet and the rats in early stages of diabetes.[25,36] Similarly, Walton reported that chronic Al exposure impairs neurites of hippocampal neurons by altering the assembly and maintenance of microtubules.[37] In addition to the generation of new neurons, structural degeneration, loss of dendritic spines, and dendritic connectivity were induced by Al exposure in hippocampal neurons.[38,39]

After new neuron generation, synapses are newly formed by increased connections between neuronal axons, synaptic integration, and the formation of neuronal dendrites and cell bodies. Long-term potentiation (LTP) is associated with synaptic integration, neuronal activity, and subsequent learning and memory formation.[40] The opening of NMDAR channels and the increase in the Ca^{2+} concentration are postsynaptically

involved in LTP.[40] NMDAR also participates in the multifaceted functions including neural plasticity, such as neuronal spine formation, neuronal migration and differentiation, and synaptogenesis.[41,42] In the hippocampus, NMDAR complexes are composed of the essential NMDAR1 subtype and auxiliary NMDAR2A and NMDAR2B subtypes.[43] The present study found that long-term diabetes did not alter the expression levels of the three major subtypes of NMDARs in the hippocampus. Al treatment did not change the expression level of NMDARs in the hippocampus in ZLC rats. The present findings are similar to those in another long-term study, in which no significant changes in NMDAR1, NMDAR2A, and NMDAR2B were found in the hippocampus in a T1DM model.[44] However, the co-existence of Al exposure and diabetes affected the NMDAR expression in the hippocampus in the ZDF–Al rats. Essential NMDAR1 was prominently reduced and auxiliary NMDAR2B was conversely increased in ZDF–Al rats. The present findings suggest that the reduction of NMDAR1 is partially correlated with the decrease of the newly generated neurons in the hippocampus, and the hypothesis is supported by results from a previous study, which indicates that the genetic modulation of NMDAR1 regulates the survival of the newly generated neurons in the early state of hippocampal neurogenesis.[45] Along with essential NMDAR1, auxiliary subtypes of NMDARs also determine the function of the NMDAR. The compositional change in the NMDAR heterotetramer is highly correlated with memory function and neurotoxicity.[46,47] Developmentally predominant NMDAR2B is replaced by NMDAR2A in the adult hippocampus, and the present study indicates that the co-existence of diabetes and Al exposure increases the level of NMDAR2B in the hippocampus in ZDF–Al rats. NMDAR2B facilitates the neurotoxicity of mature neurons in adult rats but promotes the survival of immature neurons in embryonic and neonatal rats.[48] In contrast, the expression level of NMDAR2B is reduced in the T1DM model, and this reduction is associated with the decreased electrophysiological activation of NMDAR in the hippocampus.[31] One recent study using magnetic resonance spectroscopy suggests that in addition to glutamatergic NMDARs, brain energy metabolism, such as glutamine synthesis and the glutamate–glutamine cycle, is altered in T2DM.[19] In addition, intraperitoneal Al injection also alters the brain metabolism by impairing glutamatergic and GABAergic neurotransmission.[49] Therefore, further investigations are warranted to define the effects of the co-existence of diabetes and Al-exposure on changes in the NMDAR configuration and glutamatergic and GABAergic neurotransmission.

In addition to the long-lasting hyperglycemia, brain inflammation has been considered important in the pathophysiology in diabetes-induced impairment of the hippocampal synaptic plasticity.[50] Because microglia are the main mediator of the inflammation in the brain, we investigated the effect of diabetes and Al exposure on the microglial morphology in the hippocampus. Iba-1 expression in microglia is associated with membrane ruffling and phagocytosis.[51] In this study, the long-term diabetic condition caused the altered morphology in microglia towards an activated phenotype, and cytoplasmic hypertrophy and retraction of processes were observed in the hippocampus. The numbers of Iba-1 immunoreactive microglia were not significantly different between ZDF and ZLC rats, but Iba-1 immunoreactivity significantly increased in the ZDF rats compared with the ZLC rats. The results give the clue that the diabetic condition facilitates the morphological changes (from the simple resting form to the complex activated or phagocytic form) of Iba-1 immunoreactive microglia in the dentate gyrus. In contrast, increased microglia are found in the hippocampus in the T1DM model. Notably, the lack of noticeable changes in the numbers of Iba-1 immunoreactive microglia in the T2DM model in the present study is consistent with that in previous studies with the T2DM model.[52,53] In addition, in ZDF rats aged 40 weeks, we did not microscopically observe any remarkable neurodegeneration in the hippocampus, although our recent study found that the blood–brain barrier and its related structures were morphologically changed under ultrastructural levels.[54] Al exposure did not induce significant activation of microglia in the ZLC–Al rats, but the co-existence of diabetes and Al exposure remarkably activated microglia in the hippocampus in the ZDF–Al rats. Activated microglia (in terms of the increase in Iba-1 immunoreactivity, not the number of Iba-1 immunoreactivity microglia) were easily detected in the hippocampus in ZDF–Al rats. Compared with Al exposure through drinking water, which has a weak pro-inflammatory effect, intramuscular Al vaccine adjuvant (Alhydrogel®) injection induces brain inflammation by increasing microglial cells.[55]

Conclusion

Long-term Al exposure aggravates hippocampal structural impairment in ZDF rats but not in ZLC rats. The present findings suggest that long-term Al exposure facilitates hippocampal impairment by affecting neuroblast differentiation, NMDAR expression, and microglial activation in the hippocampus.

Conflicts of interest

The authors declare that they have no conflicts of interest.

Acknowledgements

This work was supported by the Basic Science Research Program through the National Research Foundation of Korea (NRF) funded by the Ministry of Education (NRF-2015R1D1A1A01059314) and was supported by the Korea Mouse Phenotyping Project (NRF-2015M3A9D5A01076747) of the Ministry of Science, ICT and Future Planning through the National Research Foundation (NRF), Korea. This study was partially supported by the Research Institute for Veterinary Science, Seoul National University.

References

1 J. M. Forbes and M. E. Cooper, Mechanisms of diabetic complications, *Physiol. Rev.*, 2013, **93**, 137–188.

2 F. Ma, T. Wu, R. Miao, Y. Y. Xiao, W. Zhang and G. Huang, Conversion of mild cognitive impairment to dementia among subjects with diabetes: a population-based study of incidence and risk factors with five years of follow-up, *J. Alzheimer's Dis.*, 2015, **43**, 1441–1449.

3 Z. G. Li, M. Britton, A. A. Sima and J. C. Dunbar, Diabetes enhances apoptosis induced by cerebral ischemia, *Life Sci.*, 2004, **76**, 249–262.

4 Z. G. Li, W. Zhang, G. Grunberger and A. A. Sima, Hippocampal neuronal apoptosis in type 1 diabetes, *Brain Res.*, 2002, **946**, 221–231.

5 M. J. Ball, Neuronal loss, neurofibrillary tangles and granulovacuolar degeneration in the hippocampus with ageing and dementia. A quantitative study, *Acta Neuropathol.*, 1977, **37**, 111–118.

6 J. M. Duarte, Metabolic Alterations Associated to Brain Dysfunction in Diabetes, *Aging Dis.*, 2015, **6**, 304–321.

7 N. Ho, M. S. Sommers and I. Lucki, Effects of diabetes on hippocampal neurogenesis: links to cognition and depression, *Neurosci. Biobehav. Rev.*, 2013, **37**, 1346–1362.

8 C. C. Huang, C. M. Chung, H. B. Leu, L. Y. Lin, C. C. Chiu, C. Y. Hsu, C. H. Chiang, P. H. Huang, T. J. Chen, S. J. Lin, J. W. Chen and W. L. Chan, Diabetes mellitus and the risk of Alzheimer's disease: a nationwide population-based study, *PLoS One*, 2014, **9**, e87095.

9 A. Jayaraman and C. J. Pike, Alzheimer's disease and type 2 diabetes: multiple mechanisms contribute to interactions, *Curr. Diab. Rep.*, 2014, **14**, 476.

10 G. R. Sridhar, G. Lakshmi and G. Nagamani, Emerging links between type 2 diabetes and Alzheimer's disease, *World J. Diabetes*, 2015, **6**, 744–751.

11 F. Aguilar, H. Autrup, S. Barlow, L. Castle, R. Crebelli, W. Dekant, K. H. Engel, N. Gontard, D. Gott, S. Grilli, R. Gürtler, J. C. Larsen, C. Leclercq, J. C. Leblanc, F. X. Malcata, W. Mennes, M. R. Milana, I. Pratt, I. Rietjens, P. Tobback and F. Toldrá, Safety of aluminium from dietary intake scientific opinion of the panel on food additives, flavourings, processing aids and food contact materials (AFC), *EFSA J.*, 2008, **754**, 1–34.

12 Z. Z. Sun, Z. B. Chen, H. Jiang, L. L. Li, E. G. Li and Y. Xu, Alteration of Aβ metabolism-related molecules in predementia induced by AlCl3 and D-galactose, *Age*, 2009, **31**, 277–284.

13 L. Wang, J. Hu, Y. Zhao, X. Lu, Q. Zhang and Q. Niu, Effects of aluminium on β-amyloid (1–42) and secretases (APP-cleaving enzymes) in rat brain, *Neurochem. Res.*, 2014, **39**, 1338–1345.

14 C. Carvalho, N. Machado, P. C. Mota, S. C. Correia, S. Cardoso, R. X. Santos, M. S. Santos, C. R. Oliveira and P. I. Moreira, Type 2 diabetic and Alzheimer's disease mice present similar behavioral, cognitive, and vascular anomalies, *J. Alzheimer's Dis.*, 2013, **35**, 623–635.

15 C. Julien, C. Tremblay, A. Phivilay, L. Berthiaume, V. Emond, P. Julien and F. Calon, High-fat diet aggravates amyloid-beta and tau pathologies in the 3xTg-AD mouse model, *Neurobiol. Aging*, 2010, **31**, 1516–1531.

16 J. Sepulcre, M. R. Sabuncu, A. Becker, R. Sperling and K. A. Johnson, In vivo characterization of the early states of the amyloid-beta network, *Brain*, 2013, **136**, 2239–2252.

17 D. Julka, R. K. Vasishta and K. D. Gill, Distribution of aluminum in different brain regions and body organs of rat, *Biol. Trace Elem. Res.*, 1996, **52**, 181–192.

18 M. Wang, J. Chen, D. Ruan and Y. Xu, The influence of developmental period of aluminum exposure on synaptic plasticity in the adult rat dentate gyrus in vivo, *Neuroscience*, 2002, **113**, 411–419.

19 F. M. Girault, S. Sonnay, R. Gruetter and J. M. N. Duarte, Alterations of brain energy metabolism in type 2 diabetic Goto-Kakizaki rats measured in vivo by ^{13}C magnetic resonance spectroscopy, *Neurotoxic. Res.*, 2017, DOI: 10.1007/s12640-017-9821-y.

20 I. K. Hwang, S. S. Yi, Y. N. Kim, I. Y. Kim, I. S. Lee, Y. S. Yoon and J. K. Seong, Reduced hippocampal cell differentiation in the subgranular zone of the dentate gyrus in a rat model of type II diabetes, *Neurochem. Res.*, 2008, **33**, 394–400.

21 D. R. McLachlan, C. Bergeron, J. E. Smith, D. Boomer and S. L. Rifat, Risk for neuropathologically confirmed Alzheimer's disease and residual aluminum in municipal drinking water employing weighted residential histories, *Neurology*, 1996, **46**, 401–405.

22 J. R. Walton and M. X. Wang, APP expression, distribution and accumulation are altered by aluminum in a rodent model for Alzheimer's disease, *J. Inorg. Biochem.*, 2009, **103**, 1548–1554.

23 S. M. Chiroma, M. A. Mohd Moklas, C. N. Mat Taib, M. T. H. Baharuldin and Z. Amon, d-galactose and aluminium chloride induced rat model with cognitive impairments, *Biomed. Pharmacother.*, 2018, **103**, 1602–1608.

24 Y. Luo, J. Nie, Q. H. Gong, Y. F. Lu, Q. Wu and J. S. Shi, Protective effects of icariin against learning and memory deficits induced by aluminium in rats, *Clin. Exp. Pharmacol. Physiol.*, 2007, **34**, 792–795.

25 S. M. Nam, J. W. Kim, D. Y. Yoo, H. Y. Jung, J. H. Choi, I. K. Hwang, J. K. Seong and Y. S. Yoon, Reduction of adult hippocampal neurogenesis is amplified by aluminum exposure in a model of type 2 diabetes, *J. Vet. Sci.*, 2016, **17**, 13–20.

26 G. Paxinos and C. Watson, *The rat brain in stereotaxic coordinates*, Elsevier Academic Press, Amsterdam, 2007.

27 R. H. Unger, How obesity causes diabetes in Zucker diabetic fatty rats, *Trends Endocrinol. Metab.*, 1997, **8**, 276–282.

28 B. Wang, P. C. Chandrasekera and J. J. Pippin, Leptin- and leptin receptor-deficient rodent models: relevance for human type 2 diabetes, *Curr. Diabetes Rev.*, 2014, **10**, 131–145.

29 Y. T. Zhou, M. Shimabukuro, Y. Lee, K. Koyama, M. Higa, T. Ferguson and R. H. Unger, Enhanced de novo lipogenesis in the leptin-unresponsive pancreatic islets of prediabetic Zucker diabetic fatty rats: role in the pathogenesis of lipotoxic diabetes, *Diabetes*, 1998, **47**, 1904–1908.

30 S. H. Bates, R. N. Kulkarni, M. Seifert and M. G. Myers Jr., Roles for leptin receptor/STAT3-dependent and -independent signals in the regulation of glucose homeostasis, *Cell Metab.*, 2005, **1**, 169–178.

31 F. Gardoni, A. Kamal, C. Bellone, G. J. Biessels, G. M. Ramakers, F. Cattabeni, W. H. Gispent and M. Di. Luca, Effects of streptozotocin-diabetes on the hippocampal NMDA receptor complex in rats, *J. Neurochem.*, 2002, **80**, 438–447.

32 American Diabetes Association, Diagnosis and classification of diabetes mellitus, *Diabetes Care*, 2014, **37S**, 81–90.

33 L. S. Dalbøge, D. L. Almholt, T. S. Neerup, E. Vassiliadis, N. Vrang, L. Pedersen, K. Fosgerau and J. Jelsing, Characterisation of age-dependent beta cell dynamics in the male db/db mice, *PLoS One*, 2013, **8**, e82813.

34 C. A. Moores, M. Perderiset, F. Francis, J. Chelly, A. Houdusse and d R. A. Milligan, Mechanism of microtubule stabilization by doublecortin, *Mol. Cell*, 2004, **14**, 833–839.

35 J. P. Brown, S. Couillard-Després, C. M. Cooper-Kuhn, J. Winkler, L. Aigner and H. G. Kuhn, Transient expression of doublecortin during adult neurogenesis, *J. Comp. Neurol.*, 2003, **467**, 1–10.

36 S. M. Nam, J. W. Kim, D. Y. Yoo, W. Kim, H. Y. Jung, I. K. Hwang, J. K. Seong and Y. S. Yoon, Additive or synergistic effects of aluminum on the reduction of neural stem cells, cell proliferation, and neuroblast differentiation in the dentate gyrus of high-fat diet-fed mice, *Biol. Trace Elem. Res.*, 2014, **157**, 51–59.

37 J. R. Walton, Brain lesions comprised of aluminum-rich cells that lack microtubules may be associated with the cognitive deficit of Alzheimer's disease, *Neurotoxicology*, 2009, **30**, 1059–1069.

38 Z. Cao, X. Yang, H. Zhang, H. Wang, W. Huang, F. Xu, C. Zhuang, X. Wang and Y. Li, Aluminum chloride induces neuroinflammation, loss of neuronal dendritic spine and cognition impairment in developing rat, *Chemosphere*, 2016, **151**, 289–295.

39 E. Sreekumaran, T. Ramakrishna, T. R. Madhav, D. Anandh, B. M. Prabhu, S. Sulekha, P. N. Bindu and T. R. Raju, Loss of dendritic connectivity in CA1, CA2, and CA3 neurons in hippocampus in rat under aluminum toxicity: antidotal effect of pyridoxine, *Brain Res. Bull.*, 2003, **59**, 421–427.

40 K. Sakimura, T. Kutsuwada, I. Ito, T. Manabe, C. Takayama, E. Kushiya, T. Yagi, S. Aizawa, Y. Inoue, H. Sugiyama and M. Mishina, Reduced hippocampal LTP and spatial learning in mice lacking NMDA receptor ε1 subunit, *Nature*, 1995, **373**, 151–155.

41 K. A. Waters and R. Machaalani, NMDA receptors in the developing brain and effects of noxious insults, *Neurosignals*, 2004, **13**, 162–174.

42 C. Zhao, W. Deng and F. H. Gage, Mechanisms and functional implications of adult neurogenesis, *Cell*, 2008, **132**, 6451660.

43 C. Rauner and G. Köhr, Triheteromeric NR1/NR2A/NR2B receptors constitute the major N-methyl-D-aspartate receptor population in adult hippocampal synapses, *J. Biol. Chem.*, 2011, **286**, 7558–7566.

44 S. Sasaki-Hamada, H. Sacai and J. I. Oka, Diabetes onset influences hippocampal synaptic plasticity in streptozotocin-treated rats, *Neuroscience*, 2012, **227**, 293–304.

45 A. Tashiro, V. M. Sandler, N. Toni, C. Zhao and F. H. Gage, NMDA-receptor-mediated, cell-specific integration of new neurons in adult dentate gyrus, *Nature*, 2006, **442**, 929–933.

46 X. Zhao, R. Rosenke, D. Kronemann, B. Brim, S. R. Das, A. W. Dunah and K. R. Magnusson, The effects of aging on N-methyl-D-aspartate receptor subunits in the synaptic membrane and relationships to long-term spatial memory, *Neuroscience*, 2009, **162**, 933–945.

47 M. Zhou and M. Baudry, Developmental changes in NMDA neurotoxicity reflect developmental changes in subunit composition of NMDA receptors, *J. Neurosci.*, 2006, **26**, 2956–2963.

48 L. Xiao, C. Hu, C. Feng and Y. Chen, Switching of N-methyl-D-aspartate (NMDA) receptor-favorite intracellular signal pathways from ERK1/2 protein to p38 mitogen-activated protein kinase leads to developmental changes in NMDA neurotoxicity, *J. Biol. Chem.*, 2011, **286**, 20175–20193.

49 K. Saba, N. Rajnala, P. Veeraiah, V. Tiwari, R. K. Rana, S. C. Lakhotia and A. B. Patel, Energetics of excitatory and inhibitory neurotransmission in aluminum chloride model of Alzheimer's disease: reversal of behavioral and metabolic deficits by Rasa Sindoor, *Front. Mol. Neurosci.*, 2017, **10**, 323.

50 X. Tian, Y. Liu, G. Ren, L. Yin, X. Liang, T. Geng, H. Dang and R. An, Resveratrol limits diabetes-associated cognitive decline in rats by preventing oxidative stress and inflammation and modulating hippocampal structural synaptic plasticity, *Brain Res.*, 2016, **1650**, 1–9.

51 K. Ohsawa, Y. Imai, H. Kanazawa, Y. Sasaki and S. Kohsaka, Involvement of Iba1 in membrane ruffling and phagocytosis of macrophages/microglia, *J. Cell Sci.*, 2000, **113**, 3073–3084.

52 I. K. Hwang, J. H. Choi, S. M. Nam, O. K. Park, D. Y. Yoo, W. Kim, S. S. Yi, M. H. Won, J. K. Seong and Y. S. Yoon, Activation of microglia and induction of pro-inflammatory cytokines in the hippocampus of type 2 diabetic rats, *Neurol. Res.*, 2014, **36**, 824–832.

53 S. M. Nam, Y. N. Kim, D. Y. Yoo, S. S. Yi, J. H. Choi, I. K. Hwang, J. K. Seong and Y. S. Yoon, Hypothyroidism affects astrocyte and microglial morphology in type 2 diabetes, *Neural Regener. Res.*, 2013, **8**, 2458–2467.

54 S. M. Nam, D. Y. Yoo, H. J. Kwon, J. W. Kim, H. Y. Jung, D. W. Kim, H. J. Han, M. H. Won, J. K. Seong, I. K. Hwang and Y. S. Yoon, Proteomic approach to detect changes in hippocampal protein levels in an animal model of type 2 diabetes, *Neurochem. Int.*, 2017, **108**, 246–253.

55 G. Crépeaux, H. Eidi, M. O. David, Y. Baba-Amer, E. Tzavara, B. Giros, F. J. Authier, C. Exley, C. A. Shaw, J. Cadusseau and R. K. Gherardi, Non-linear dose-response of aluminium hydroxide adjuvant particles: Selective low dose neurotoxicity, *Toxicology*, 2017, **375**, 48–57.